

# Random numbers and random matrices: Quantum chaos meets number theory

Todd Timberlake<sup>a)</sup>

*Department of Physics, Astronomy, and Geology, Berry College, Mount Berry, Georgia 30149-5004*

(Received 3 August 2005; accepted 31 March 2006)

The statistical analysis of the eigenvalues of quantum systems has become an important tool in understanding the connections between classical and quantum physics. The statistical properties of the eigenvalues of a quantum system whose classical counterpart is integrable match those of random numbers. The eigenvalues of a chaotic classical system have statistical properties like those of the eigenvalues of random Hermitian matrices. The statistical properties of random numbers and eigenvalues of random Hermitian matrices are examined and the connection between these properties and the statistics of eigenvalues of quantum systems is illustrated, using the quantum standard map as an example. The relevance of these ideas to some problems in the theory of prime numbers is explored. © 2006 American Association of Physics Teachers.  
[DOI: 10.1119/1.2198883]

## I. INTRODUCTION

Classical systems can exhibit qualitatively different types of motion: chaotic motion, which exhibits sensitive dependence on initial conditions, and regular motion which does not. In quantum mechanics, sensitive dependence on initial conditions is not possible due to the Heisenberg uncertainty principle which prevents a quantum particle from having well-defined initial conditions. In this sense, there is no chaos in quantum mechanics. However, in the last 30 years much research has gone into investigating whether or not there are any qualitative differences between quantum systems whose classical counterparts are chaotic and those whose classical counterparts are regular. One of the most important discoveries in this area of quantum chaos has to do with the statistics of eigenvalue sequences.

In the 1950s Eugene Wigner recognized the importance of eigenvalue statistics when he studied the distribution of spacings between energy levels of highly excited nuclei.<sup>1</sup> He found that the nuclear energy levels were statistically similar to the eigenvalues of a random Hermitian matrix. It is not surprising that the nuclear energy levels have properties similar to the eigenvalues of a Hermitian matrix, because the Hamiltonian is represented by a Hermitian matrix. What is surprising is that their behavior should mimic that of a random matrix. Much experimental data on nuclear energy levels has been shown to fit the predictions of random matrix theory.<sup>2</sup>

It would be many years before Wigner's pioneering work on eigenvalue statistics found application in the field of quantum chaos. In 1977 Berry and Tabor<sup>3</sup> proposed that the sequence of energy levels for a generic quantum system with integrable classical counterpart should have statistical properties like those of random numbers. In 1984 Bohigas, Gianoni, and Schmit<sup>4</sup> provided evidence that the quantum energy level sequences of systems with chaotic classical counterparts have statistical properties that fit the predictions of random matrix theory. Much experimental and numerical evidence has supported these conjectures, and some authors have taken the statistical properties of the spectra as the definition of quantum chaos although such a definition is not universally accepted.

The statistics of random sequences has also found applications in areas outside of physics. In number theory, for

example, the sequence of prime numbers is statistically similar to a sequence of random numbers,<sup>5</sup> and the imaginary parts of the nontrivial zeros of the Riemann zeta function (numbers that are intimately tied to the detailed distribution of prime numbers) have statistical properties that fit the predictions of random matrix theory.<sup>6</sup>

The goal of this paper is to illustrate how the statistical properties of the eigenvalues of a quantum system change as its classical counterpart makes a transition from regular to chaotic motion. I focus on the nearest neighbor spacing distribution, which is one of the simplest tools for studying eigenvalue statistics. Section II describes the nearest neighbor spacing distributions for random numbers and random matrix eigenvalues and illustrates the validity of these results with numerical computations. Section III illustrates how the nearest neighbor spacing distribution of a quantum system changes as its classical counterpart becomes chaotic. Section IV explores the connections between these ideas and the theory of prime numbers.

## II. RANDOM NUMBERS AND MATRICES

The idea of the nearest neighbor spacing distribution is to analyze how the spacings between consecutive numbers in a number sequence fluctuate about the average spacing. This analysis requires that there be a well-defined average spacing. But the average spacing (averaged over many consecutive spacings, but not over the entire sequence) may not be uniform throughout the sequence. If this local average changes significantly on the scale of a single spacing, then there is no hope of separating the large-scale variation in the spacings from the local fluctuations. However, if the local average varies only on scales that are large compared to a single spacing, then the effects of this variation can be separated from the local fluctuations using a process called *unfolding*.

Let  $E$  represent a number in the sequence. The average density of the numbers in the sequence (the reciprocal of the average spacing) as a function of  $E$  is represented by  $\bar{\rho}(E)$ . The sequence can be unfolded using the average level staircase function,

$$\bar{\eta}(E) = \int_{-\infty}^E dE' \bar{\rho}(E'), \quad (1)$$

which tells us how many members of our sequence are less than  $E$  on average. The unfolded sequence is given by

$$e_i = \bar{\eta}(E_i), \quad (2)$$

where the index  $i$  labels the numbers in the sequence. The unfolded sequence  $(e_1, e_2, \dots, e_N)$  will have a uniform average spacing equal to one, although individual spacings will fluctuate about this average. The nearest neighbor spacing distribution is constructed by computing the differences between consecutive numbers  $e_{i+1} - e_i$ , organizing these spacings into bins, and constructing a histogram to obtain a picture of how the individual spacings fluctuate about the average.

### A. Random numbers

A standard random number generator<sup>7</sup> yields a number in the interval  $[0, 1)$ . The probability distribution for an ideal random number generator is uniform on this interval (all values on the interval are equally likely to be produced). Random numbers are uncorrelated, which means the probability of generating a particular value with a random number generator is independent of the values that have been generated previously. Therefore, a list of numbers produced by a random number generator has uniform average density and requires no unfolding. To calculate the spacings we need only sort the numbers, take the difference between consecutive numbers, and then scale these differences so that the mean spacing is one.

### B. Random matrices

Random matrices are not simply matrices whose elements are random numbers. The matrix elements must satisfy the symmetries of the matrix. I will discuss only random Hermitian matrices, because Hermitian matrices represent physical observables in quantum mechanics. The symmetry of these matrices puts severe restrictions on the matrix elements, because the elements of a Hermitian matrix  $\hat{H}$  satisfy  $H_{mn} = H_{nm}^*$ . If the matrix  $\hat{H}$  represents a Hamiltonian of a physical system, it may have additional symmetries related to the symmetries of the system. In particular, if a system (without spin-1/2 interactions) is symmetric under time-reversal, then its Hamiltonian can always be represented as a real symmetric matrix.<sup>8</sup> If the system is not symmetric under time-reversal, the Hamiltonian will be a complex Hermitian matrix.

These symmetries play an important role in determining the probability distribution for a random matrix.<sup>9,10</sup> The probability distribution must be invariant under a change of basis. Thus  $P(\hat{H}) = P(\hat{H}')$ , where  $\hat{H}'$  is obtained from  $\hat{H}$  by a change of basis. Any change of basis must preserve the symmetry of the matrix. The symmetry of real symmetric matrices is preserved by orthogonal transformations ( $\hat{H}' = \hat{O}\hat{H}\hat{O}^T$ , where  $\hat{O}$  is an orthogonal matrix), and the symmetry of complex Hermitian matrices is preserved by unitary transformations ( $\hat{H}' = \hat{U}\hat{H}\hat{U}^\dagger$  with  $\hat{U}$  a unitary matrix). Thus we must consider two separate ensembles of random matrices: real symmetric random matrices whose probability distribution is

invariant under orthogonal transformations (the Gaussian orthogonal ensemble), and complex Hermitian random matrices whose probability distribution is invariant under unitary transformations (the Gaussian unitary ensemble). In both cases,  $P(\hat{H})$  depends only on traces of powers of  $\hat{H}$  to ensure that  $P(\hat{H})$  is invariant under the appropriate transformation. If we also require that the matrix elements be statistically independent (to the extent allowed by the symmetry of the matrix), then the distribution is further restricted and

$$P(\hat{H}) = C \exp(-a \text{Tr} \hat{H}^2), \quad (3)$$

where  $C$  and  $a$  are constants and  $\text{Tr} \hat{H}^2$  is the trace of the square of the matrix. For a  $2 \times 2$  real symmetric matrix

$$P(\hat{H}) = C \exp(-a(h_{11}^2 + h_{22}^2 + 2h_{12}^2)), \quad (4)$$

which shows that each matrix element is Gaussian random and the variance of the off-diagonal element is one-half that of the diagonal elements. To construct an  $N \times N$  Gaussian orthogonal ensemble matrix, we choose the diagonal elements of the matrix  $H_{mn}$  from a Gaussian distribution with mean zero and variance one. The elements above the diagonal ( $H_{mn}$ , with  $m < n$ ) should be Gaussian-random with mean zero and variance one half. The elements below the diagonal are generated from the symmetry of the matrix  $H_{mn} = H_{nm}^*$ . For a Gaussian unitary ensemble matrix the diagonal elements are also Gaussian-random with mean zero and variance one. The elements above the diagonal have independent real and imaginary parts that are each Gaussian random with mean zero and variance one half. The elements below the diagonal are obtained from  $H_{mn} = H_{nm}^*$ .

Once the random matrix has been created, its eigenvalues can be obtained numerically. Unlike a sequence of random numbers, the eigenvalues of a random matrix are not distributed uniformly. Wigner derived the average density of eigenvalues,<sup>11</sup> now known as the *Wigner semicircle law*

$$\bar{\rho}(E) = \begin{cases} \frac{1}{\pi} \sqrt{2N - E^2}, & |E| < \sqrt{2N} \\ 0, & |E| > \sqrt{2N}, \end{cases} \quad (5)$$

which holds for both Gaussian orthogonal and Gaussian unitary ensemble matrices in the limit  $N \rightarrow \infty$ . Figure 1(a) shows the agreement between the calculated density of the eigenvalues for a  $3000 \times 3000$  Gaussian orthogonal ensemble matrix and the Wigner semicircle law. The Wigner semicircle law can be integrated to obtain the average level staircase function

$$\bar{\eta}(E) = \frac{1}{2\pi} \left( E \sqrt{2N - E^2} + 2N \sin^{-1} \left( \frac{E}{\sqrt{2N}} \right) + \pi N \right), \quad (6)$$

which can be used to unfold the eigenvalues using Eq. (2). The unfolded eigenvalues will then be distributed uniformly, on average, with mean spacing one. After the eigenvalues have been unfolded, they can be sorted and the differences between consecutive eigenvalues can be computed.

### C. Level spacing distributions

Random numbers are uncorrelated and this property determines the distribution of spacings between nearest neighbors in an ordered random number sequence.<sup>12</sup> Given a number  $E$  in the sequence, the probability  $P(s)ds$  that the next number

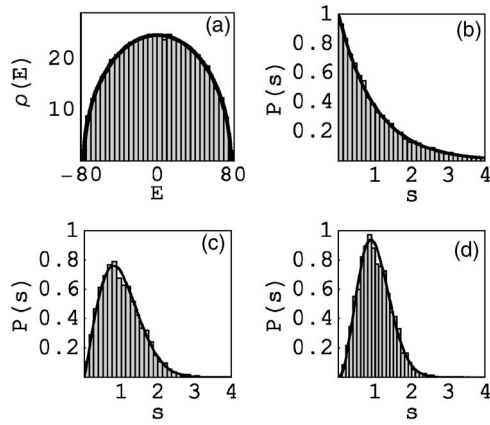


Fig. 1. Statistical distributions of random numbers and eigenvalues of random matrices. The histogram in (a) shows the distribution of eigenvalues for an  $N \times N$  real symmetric random matrix with  $N=3000$ . The solid curve is the Wigner semicircle law, Eq. (5). The histogram in (b) shows the nearest neighbor spacing distribution for 10 000 random numbers. The solid curve shows the Poisson distribution, Eq. (8). The histogram in (c) shows the nearest neighbor spacing distribution for the unfolded eigenvalues of a random real symmetric matrix ( $N=3000$ ) and the solid curve shows the Wigner Gaussian orthogonal ensemble distribution, Eq. (9). The histogram in (d) shows the nearest neighbor spacing distribution for the unfolded eigenvalues of a random complex Hermitian matrix ( $N=3000$ ) and the solid curve shows the Wigner Gaussian unitary ensemble distribution, Eq. (10).

in the sequence lies between  $E+s$  and  $E+s+ds$  is proportional to the probability that there is no level between  $E$  and  $E+s$ . Thus

$$P(s)ds = a \left( 1 - \int_0^s P(s')ds' \right), \quad (7)$$

where  $a$  is a constant. The integral equation (7) can be solved to show that the nearest neighbor spacing distribution for random numbers is the Poisson distribution

$$P(s) = e^{-s}, \quad (8)$$

where  $P(s)$  has been normalized so that the mean spacing is one. Figure 1(b) shows the agreement between the computed nearest neighbor spacing distribution for 10 000 random numbers and the Poisson distribution. Note that the Poisson distribution is peaked at  $s=0$ , indicating that small spacings are very likely in a sequence of random numbers. This tendency of random numbers to clump together is called *level clustering*.

The theoretical spacing distributions for the unfolded eigenvalues of random matrices are not so simple. The limiting spacing distributions for an  $N \times N$  random matrix as  $N \rightarrow \infty$  involve complicated Taylor series expansions.<sup>13</sup> Wigner derived the spacing distributions for ensembles of  $2 \times 2$  random matrices<sup>11,14</sup> and these distributions differ only slightly from the limiting distributions for  $N \rightarrow \infty$ . For most purposes it is sufficient to use the Wigner distributions to describe the nearest neighbor spacing distribution for eigenvalues of random Hermitian matrices.

The Wigner distribution for unfolded eigenvalues of a Gaussian orthogonal ensemble matrix is

$$P(s) = \frac{\pi}{2} s \exp\left(-\frac{\pi}{4} s^2\right). \quad (9)$$

Figure 1(c) shows the agreement between the computed nearest neighbor spacing distribution for the unfolded eigenvalues of a  $3000 \times 3000$  Gaussian orthogonal ensemble matrix and the corresponding Wigner distribution. Note that the Wigner distribution for the Gaussian orthogonal ensemble decreases linearly to zero as  $s \rightarrow 0$ . For this reason the eigenvalues of a Gaussian orthogonal ensemble matrix are said to exhibit *linear level repulsion*. The eigenvalues of a Gaussian orthogonal ensemble matrix are correlated and tend to repel each other, leading to the absence of small spacings in the nearest neighbor spacing distribution.

For Gaussian unitary ensemble matrices the Wigner distribution is

$$P(s) = \frac{32}{\pi^2} s^2 \exp\left(-\frac{4}{\pi} s^2\right), \quad (10)$$

where again Eq. (10) is exact for  $N=2$  and close for  $N \rightarrow \infty$ . Figure 1(d) shows the agreement between the computed nearest neighbor spacing distribution for the unfolded eigenvalues of a  $3000 \times 3000$  Gaussian unitary ensemble matrix and the corresponding Wigner distribution. In this case the Wigner distribution falls off quadratically as  $s \rightarrow 0$ , so the eigenvalues of such a matrix are said to exhibit *quadratic level repulsion*.

### III. QUANTUM CHAOS

As mentioned in Sec. I, the eigenvalues of quantum systems whose classical counterparts are regular have Poisson level spacing distributions, while the eigenvalues of quantum systems with chaotic classical counterparts have random matrix level spacing distributions. A classical system that undergoes a transition from regular motion to chaos as some parameter is varied should have a quantum counterpart whose eigenvalues undergo a transition from Poisson to random matrix statistics for the same variation of the parameter. These transitions are illustrated in the following.

#### A. Classical standard map

Hamiltonian (conservative) systems with one degree of freedom cannot be chaotic. The simplest systems that can exhibit classical chaos are one-dimensional potentials subject to a periodic driving force. Often the dynamics of a periodic system can be reduced to a mapping function that maps the location of a trajectory in phase space at time  $t_0$  to its location at time  $t_0+T$ , where  $T$  is the period of the driving field. For a rigid rotor subject to periodic delta-function kicks, the mapping function, known as the standard map,<sup>15</sup> is

$$\begin{pmatrix} q' \\ p' \end{pmatrix} = \begin{pmatrix} q + p - \frac{k}{2\pi} \sin(2\pi q) \\ p - \frac{k}{2\pi} \sin(2\pi q) \end{pmatrix} \text{mod } 1, \quad (11)$$

where  $q$  and  $p$  are dimensionless phase space variables and  $k$  is a dimensionless parameter that controls the nonlinearity of the map. Both  $q$  and  $p$  are periodic coordinates with period one, that is,  $q$  is equivalent to  $q+1$ . Therefore the phase space for this map is a 2-torus with area one in dimensionless units.

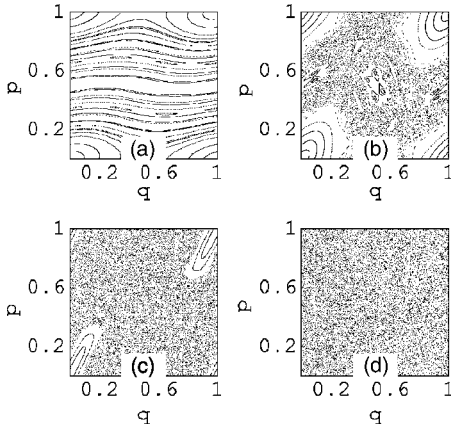


Fig. 2. Strobe plots for the classical standard map with (a)  $k=0.3$ , (b)  $k=1.5$ , (c)  $k=3.9$ , and (d)  $k=7$ . At low values of  $k$  the classical trajectories are almost all regular. As  $k$  is increased a larger portion of the phase space becomes chaotic. At  $k=7$  the entire phase space is chaotic.

If we start with some initial location in phase space and repeatedly iterate the mapping function, we produce a set of points called a trajectory. This set of points shows the location of the classical system in phase space after each kick and provides a picture of the motion similar to what one might see when watching a moving object illuminated by a strobe light. A plot composed of trajectories for a variety of initial conditions scattered throughout the phase space is therefore called a strobe plot. A strobe plot provides an overview of the dynamics of the map in all parts of the phase space. Figure 2 shows strobe plots for the standard map with various values of the nonlinearity parameter  $k$ . Continuous curves and ordered sequences of points such as those seen in Fig. 2(a) indicate regions of regular motion. A random scatter of points [such as that seen throughout Fig. 2(d)] indicates a region of chaotic motion. It is clear from Figs. 2(a)–2(d) that the standard map makes a transition from regular motion to chaos as  $k$  is increased from 0.3 to 7. A more detailed introduction to the dynamics of the standard map can be found in Ref. 16.

## B. Quantum standard map

As mentioned, the standard map represents the dynamics of a system that is subject to a periodic driving force. In such a system the Hamiltonian depends explicitly on time and energy is not conserved because the Hamiltonian is not invariant under infinitesimal time translations  $t \rightarrow t + \delta t$ . Therefore, to analyze the quantum dynamics of the standard map we cannot take the usual approach of finding energy eigenvalues and eigenvectors. However, the Hamiltonian of a periodically driven system is invariant under the discrete time translation  $t \rightarrow t + T$ , where  $T$  is the period of the driving force. Because of this symmetry, it is possible to construct an operator whose eigenvalues and eigenvectors will characterize the dynamics of the system in much the same way that the eigenvalues and eigenvectors of the Hamiltonian characterize the dynamics of energy-conserving systems. The operator that serves this purpose is the Floquet operator,  $\hat{U}(t, t+T) = \hat{U}$ , which is the unitary time evolution operator that transforms the wavefunction at time  $t$  into the wavefunc-

tion at time  $t+T$  (so  $\hat{U}\psi(t) = \psi(t+T)$ ). The Floquet operator is the quantum counterpart of the classical mapping function.

The eigenvalues of the Floquet operator have the form  $\lambda = \exp(-i\phi)$  because the Floquet operator is unitary and must have eigenvalues of unit modulus. The quantity  $\phi$  is called a quasienergy (or eigenphase) and is only defined modulo  $2\pi$  because  $\exp(-i\phi) = \exp(-i(\phi \pm 2\pi n))$  for any integer  $n$ . The discussion in Sec. II B referred to the eigenvalues of Hermitian matrices, in contrast to our present discussion of *eigenphases* associated with unitary matrices. An ensemble of random unitary matrices is known as a *circular ensemble*. As with random Hermitian matrices, there are different classifications of random unitary matrices based on symmetry: the circular orthogonal ensemble and the circular unitary ensemble. The nearest neighbor spacing distribution for the eigenphases of circular orthogonal and circular unitary ensemble matrices follow the same distributions as the eigenvalues of Gaussian orthogonal and Gaussian unitary ensemble matrices, respectively.<sup>17</sup> Because the standard map is time-reversal invariant, we expect the nearest neighbor spacing distribution of the quasienergies for the quantum standard map to undergo a transition from Poisson statistics at low values of  $k$  to circular/Gaussian orthogonal ensemble statistics at high values of  $k$ .

To find the quasienergies for the quantized standard map we must first construct the Floquet operator  $\hat{U}$ . The construction of a unitary evolution operator from a classical map is subtle; the result for the the standard map is<sup>18</sup>

$$(U_N)_{j'j} = \langle q_{j'} | \hat{U}_N | q_j \rangle = \frac{1}{\sqrt{N}} \exp \left[ \frac{i\pi}{N} (j' - j)^2 + \frac{ikN}{2\pi} \cos \left( \frac{2\pi j}{N} \right) \right], \quad (12)$$

where  $|q_j\rangle$  is a discrete position eigenstate with eigenvalue  $q_j = j/N$  and  $j = 0, 1, \dots, N-1$ . The number  $N$  of discrete position eigenstates determines the size of the Floquet matrix. Because the phase space is a 2-torus, the wavefunctions must satisfy periodic boundary conditions:  $\psi(q+j) = \psi(q)$  and  $\hat{\psi}(p+k) = \hat{\psi}(p)$ , where  $j$  and  $k$  are integers. The effective value of Planck's constant is  $\hbar = 1/N$ , because the number of quantum states is equal to the area of the phase space divided by  $\hbar$ , so the classical limit  $\hbar \rightarrow 0$  corresponds to  $N \rightarrow \infty$ .<sup>18</sup> To calculate the quasienergies we choose a value for  $N$ , construct the Floquet matrix according to Eq. (12), and numerically determine the eigenvalues  $\lambda_\alpha$  where  $\alpha = 1, 2, \dots, N$ . The quasienergies are given by  $\phi_\alpha = -\text{Im}[\ln \lambda_\alpha]$ . The quasienergies (modulo  $2\pi$ ) will be distributed roughly uniformly over the interval 0 to  $2\pi$ .

Because this system is symmetric under the parity transformation, the eigenstates of the Floquet operator must satisfy  $\psi_\alpha(-q_j) = \pm \psi_\alpha(q_j)$ , with the plus sign for even eigenstates and the minus sign for odd eigenstates. Recall that the wavefunction must satisfy periodic boundary conditions, so  $\psi(-q_j) = \psi(1 - q_j) = \psi(q_{N-j})$  for any integer  $j$ . Thus the Floquet eigenstates will satisfy  $\psi(q_{N-j}) = \pm \psi(q_j)$ . Because parity is a good quantum number for this system, the quasienergies obtained by diagonalizing the Floquet matrix form a mixture of two independent sequences. The mixing of two independent Gaussian orthogonal ensemble sequences causes an increase in the number of small spacings and thus leads to a nearest neighbor spacing distribution that does not fit Eq.

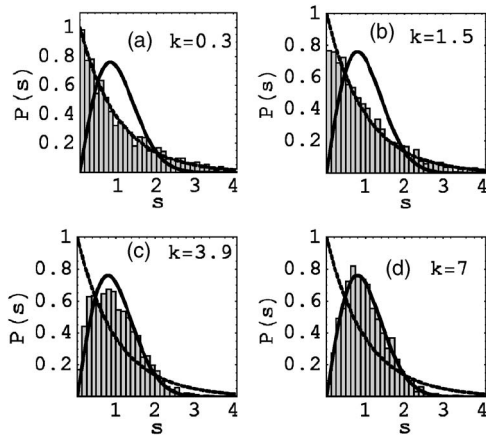


Fig. 3. Nearest neighbor spacing distributions for states of like parity for the quantum standard map with (a)  $k=0.3$ , (b)  $k=1.5$ , (c)  $k=3.9$ , and (d)  $k=7$ . Each distribution represents the spacings of 2000 eigenvalues. In each plot the dashed curve shows the Poisson distribution, Eq. (8), and the solid curve shows the Wigner Gaussian orthogonal ensemble distribution, Eq. (9).

(9).<sup>19</sup> To clearly illustrate the transition from Poisson statistics to random matrix statistics, it is important that only spacings between eigenvalues of states with the same parity be used. Therefore we must separate the states of even and odd parity before determining the nearest neighbor spacings. If  $N$  is even, the sum  $\sum_{i=0}^{N/2} |\psi(q_i) + \psi(q_{N-i})|^2$  will be zero for odd states but greater than two for even states. This criterion can be used to identify the even and odd eigenstates. The spacings between quasienergies of like parity can then be calculated, and then both sets of spacings can be recombined to produce a nearest neighbor spacing distribution histogram.

Figure 3 shows the nearest neighbor spacing distribution for quasienergies of like parity at various values of  $k$ . There is a clear transition from Poisson statistics at  $k=0.3$  to Gaussian orthogonal ensemble statistics at  $k=7$ . Note that at  $k=0$  the nearest neighbor spacing distribution is not Poissonian, but has an excess of small spacings. This deviation from Poisson statistics is typical of one-dimensional systems without time-dependent driving forces and arises because of number-theoretical degeneracies, which are eliminated when  $k$  is increased to 0.3. A comparison between Figs. 2 and 3 shows that the transition from Poisson statistics to random matrix statistics in the eigenvalues of the quantum system parallels the transition from regular motion to chaos in the classical system.

#### IV. NUMBER THEORY

The statistical properties of number sequences have helped to shed light on important problems in number theory, particularly in the study of prime numbers. The primes (2, 3, 5, 7, 11, ...) are thought to be distributed randomly among the integers, and their nearest neighbor spacing distribution provides evidence that prime numbers are statistically random. Before the nearest neighbor spacing distribution for primes can be calculated, the sequence of primes must first be unfolded. The density of primes near the  $n$ th prime is  $\bar{\rho}(p_n) = 1/\ln(p_n)$ , as originally observed by Gauss.<sup>20</sup> Figure 4(a) shows the agreement between the numerically computed

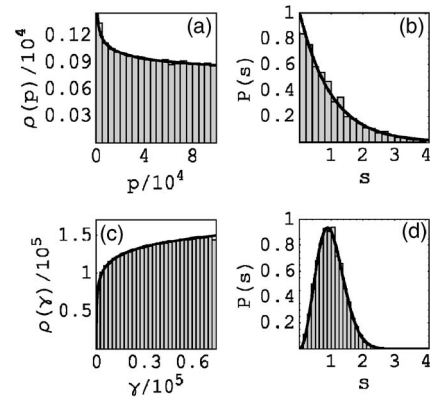


Fig. 4. Number theoretical distributions. In (a) the number density of the primes is compared to the prediction of Gauss (solid line). In (b) the nearest neighbor spacing distribution for primes is compared to the Poisson distribution of Eq. (8) (solid line). In (c) the number density of zeta zeros is compared to the prediction of Eq. (16) (solid line). In (d) the nearest neighbor spacing distribution for zeta zeros is compared to the Wigner Gaussian unitary ensemble distribution of Eq. (10) (solid line). The values of the zeta zeros were computed by Andrew Odlyzko and are available from Ref. 30.

density of the first 10 000 primes and Gauss' formula. By integrating this density we find that the average level staircase function for the primes is

$$\bar{\eta}(p_n) = \text{Li}(p_n), \quad (13)$$

where

$$\text{Li}(x) = \int_0^x \frac{dt}{\ln(t)} \quad (14)$$

is the log integral function. Thus  $\text{Li}(x)$  gives the approximate number of primes less than  $x$ . The function  $\pi(x)$  that gives the exact number of primes less than  $x$  is called the prime counting function. The fact that  $\pi(x)$  tends asymptotically to  $\text{Li}(x)$  is the essence of the famous prime number theorem proved independently by Hadamard and de la Vallée Poussin in 1896.<sup>21</sup>

The unfolded primes are given by  $e_n = \text{Li}(p_n)$ . If the primes are statistically random, then the nearest neighbor spacing distribution for the unfolded primes should fit the Poisson distribution. If the nearest neighbor spacing distribution is computed for the first 10 000 primes, the result looks somewhat Poissonian but does not match the Poisson distribution very well. In particular, there is a shortage of small spacings. However, the nearest neighbor spacing distribution for larger primes does match the Poisson distribution. Figure 4(b) shows the nearest neighbor spacing distribution for primes  $p_n$  where  $n$  ranges from  $10^{12}$  to  $10^{12} + 10^4$ . Note that the density  $\bar{\rho}(p)$  changes very little over this range of primes, so it is not necessary to go through the unfolding procedure before computing the nearest neighbor spacing distribution. Instead, the spacings can be computed using the actual primes and then scaled so that the average spacing is one. The spacing distribution for these large primes fits the Poisson distribution very well. The general trend is that larger primes follow Poisson statistics more closely, indicating that the nearest neighbor spacing distribution for the first  $N$  primes will approach the Poisson distribution as  $N \rightarrow \infty$ . The fact that the prime spacing distribution asymptotically approaches the Poisson distribution indicates that primes are randomly dis-

tributed (aside from the obvious fact that they are integers, and all but one are odd). Furthermore, it indicates that if the prime numbers are eigenvalues of some quantum system, then the classical counterpart of that system should be integrable. This idea has led to an attempt to formulate a one-dimensional potential whose quantum eigenvalues are (approximately) the prime numbers.<sup>22</sup>

Although the prime counting function  $\pi(x)$  is approximated by  $\text{Li}(x)$ , the detailed behavior of  $\pi(x)$  depends on a set of quantities known as the nontrivial zeros of the Riemann zeta function. The Riemann zeta function<sup>23</sup> for integer and real  $z > 1$  is

$$\zeta(z) = \sum_{n=1}^{\infty} \frac{1}{n^z} = \prod_p \frac{1}{1-p^{-z}}, \quad (15)$$

where the product on the right-hand side is over all primes  $p$ . The equivalence of the sum and product in Eq. (15) was shown by Euler in 1737.<sup>24</sup> Riemann extended the definition of the zeta function to the complex plane ( $z \neq 1$ ) using analytic continuation.<sup>25</sup> The Riemann zeta function has trivial zeros at the negative even integers. The rest of the zeros of the Riemann zeta function are nontrivial and lie in a strip of the complex plane bounded by the lines  $\text{Re } z=0$  and  $\text{Re } z=1$ . Riemann derived an explicit formula for  $\pi(x)$  that involves a sum over the nontrivial zeros. He also stated a conjecture that all of the nontrivial zeros have  $\text{Re } z=1/2$ . This relation is the famous Riemann hypothesis, which is one of the greatest unsolved problems in mathematics and the subject of several recent popular books.<sup>26,27</sup>

One approach to proving the Riemann hypothesis exploits a possible connection between the Riemann hypothesis and quantum mechanics. The idea is to prove that all nontrivial zeros of the Riemann zeta function are of the form  $1/2+i\gamma$ , where  $\gamma$  is a real number (hereafter I will refer to the  $\gamma$  values as zeta zeros). The Hilbert-Pólya conjecture is that the zeta zeros are eigenvalues of some Hermitian operator and are thus real, so if this conjecture is true so is the Riemann hypothesis. In quantum mechanics Hermitian operators represent physical observables. Thus perhaps the zeta zeros are the energy eigenvalues of a Hamiltonian. What kind of system would have the zeta zeros as its eigenvalues? The answer comes from analyzing the nearest neighbor spacing distribution of the zeta zeros.

The density of the zeta zeros is given by<sup>6</sup>

$$\bar{\rho}(\gamma_n) = \frac{1}{2\pi} \ln\left(\frac{\gamma_n}{2\pi}\right), \quad (16)$$

where  $\gamma_n$  is the  $n$ th positive zeta zero. Figure 4(c) shows the agreement between the computed density of the first 100 000 zeta zeros and the prediction of Eq. (16). The density can be integrated to find the average level staircase function, which provides a formula for the unfolded zeta zeros:

$$e_n = \frac{1}{2\pi} \gamma_n \left( \ln\left(\frac{\gamma_n}{2\pi}\right) - 1 \right). \quad (17)$$

The nearest neighbor spacing distribution for the first 100 000 unfolded zeta zeros is close to the Gaussian unitary ensemble distribution, Eq. (10), but is not a perfect fit.<sup>6</sup> As with the primes, though, the fit becomes better for larger zeta zeros. Figure 4(d) shows the nearest neighbor spacing distribution for the zeta zeros with  $n$  ranging from  $10^{22}$  to  $10^{22}$

+  $10^4$  [with no unfolding because  $\bar{\rho}(\gamma_n)$  is essentially constant in this range]. The fit to the Gaussian unitary ensemble distribution is very good. This fit implies that if the zeta zeros are energy eigenvalues of some quantum system, the system should be chaotic. Moreover, it tells us that the system is not time-reversal invariant. These conditions fall well short of actually producing a system whose eigenvalues are the zeta zeros (and thus proving the Riemann hypothesis), but indicate where to look for such a system.

## V. SUMMARY

The eigenvalues of a quantum system whose classical counterpart is integrable are uncorrelated, exhibit level clustering, and have statistical properties similar to those of random numbers. In contrast, the eigenvalues of a quantum system whose classical counterpart is chaotic are strongly correlated, exhibit level repulsion, and are statistically similar to the eigenvalues of random matrices. For the standard map, which makes a transition from classical integrability to chaos as a parameter is varied, the eigenvalues show a corresponding transition from random number statistics to random matrix statistics. This difference of the eigenvalue statistics is one of the most important features that distinguishes a quantum system whose classical counterpart is chaotic from a quantum system whose classical counterpart is regular. The statistical properties of random numbers and random matrix eigenvalues are also of interest in connection with the distribution of prime numbers and the zeros of the Riemann zeta function, which indicates intriguing connections between quantum mechanics and number theory.

Readers who wish to further explore this material are encouraged to do the computations discussed in this paper. A MATHEMATICA notebook, which includes some additional computations not discussed in this paper, is available for that purpose.<sup>28</sup> Much more detail about these topics can be found in books on random matrix theory,<sup>9</sup> quantum chaos,<sup>10,29</sup> and the Riemann zeta function.<sup>23,25,27</sup>

## ACKNOWLEDGMENT

The author would like to thank Andrew Oldyko for allowing the use of his tables of zeta zeros.

<sup>a</sup>Electronic mail: timberlake@berry.edu

<sup>1</sup>See Wigner's papers reprinted in *Statistical Theories of Spectra: Fluctuations*, edited by C. E. Porter (Academic, New York, 1965).

<sup>2</sup>R. U. Haq, A. Pandey, and O. Bohigas, "Fluctuation properties of nuclear energy levels: Do theory and experiment agree?," *Phys. Rev. Lett.* **48**, 1086–1089 (1982).

<sup>3</sup>M. V. Berry and M. Tabor, "Level clustering in the regular spectrum," *Proc. R. Soc. London, Ser. A* **356**, 375–394 (1977).

<sup>4</sup>O. Bohigas, M. J. Giannoni, and C. Schmit, "Characterization of chaotic quantum spectra and universality of level fluctuation laws," *Phys. Rev. Lett.* **52**, 1–4 (1984).

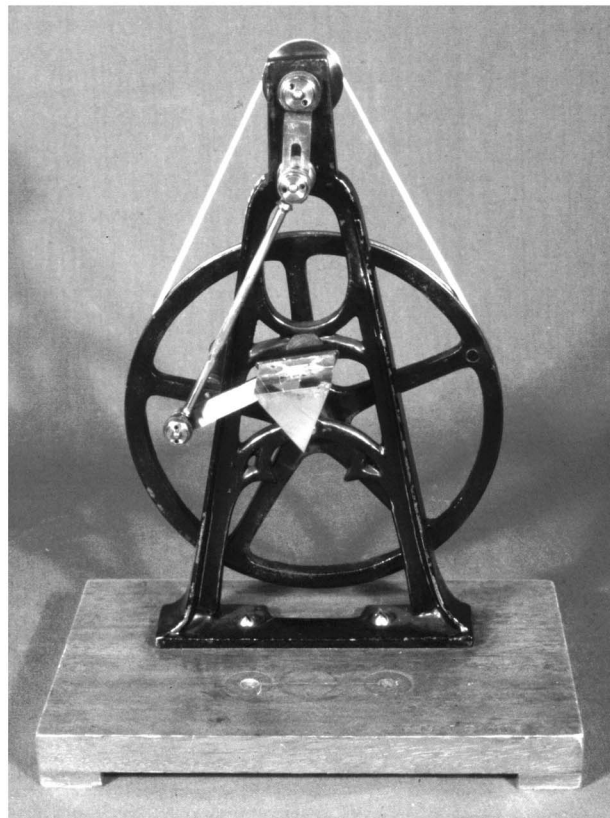
<sup>5</sup>C. E. Porter, "Fluctuations of quantal spectra," in *Statistical Theories of Spectra: Fluctuations*, edited by C. E. Porter (Academic, New York, 1965), pp. 2–87.

<sup>6</sup>A. M. Odlyzko, "On the distribution of spacings between zeros of the zeta function," *Math. Comput.* **48**, 273–308 (1987).

<sup>7</sup>Random number generators produce pseudorandom numbers, but I will ignore this distinction.

<sup>8</sup>Systems with time-reversal symmetry and spin-1/2 interactions have Hamiltonians that can be represented by real quaternion matrices, but I will not consider these here.

- <sup>9</sup>M. L. Mehta, *Random Matrices* (Elsevier Academic, San Diego, 2004), 3rd ed., pp. 33–49.
- <sup>10</sup>Fritz Haake, *Quantum Signatures of Chaos* (Springer-Verlag, Berlin, 2001), 2nd ed., pp. 48–51.
- <sup>11</sup>E. P. Wigner, “Statistical properties of real symmetric matrices with many dimensions,” *Canadian Mathematical Congress Proceedings* (University of Toronto Press, Toronto, Canada, 1957), pp. 174–184. Reprinted in Ref. 1.
- <sup>12</sup>Reference 10, pp. 123–124.
- <sup>13</sup>Reference 10, pp. 69–78.
- <sup>14</sup>Reference 10, pp. 51–54.
- <sup>15</sup>Boris V. Chirikov, “A universal instability of many dimensional oscillator systems,” *Phys. Rep.* **52**, 263–379 (1979).
- <sup>16</sup>Todd Timberlake, “A computational approach to teaching conservative chaos,” *Am. J. Phys.* **72**, 1002–1007 (2004).
- <sup>17</sup>See p. 646 of Ref. 9.
- <sup>18</sup>Arnd Bäcker, “Numerical aspects of eigenvalue and eigenfunction computations for chaotic quantum systems,” in *The Mathematical Aspects of Quantum Maps*, edited by M. D. Esposti and S. Graffi (Springer-Verlag, New York, 2003), pp. 91–144.
- <sup>19</sup>David L. Kaufman, Ioan Kosztin, and Klaus Schulten, “Expansion method for stationary states of quantum billiards,” *Am. J. Phys.* **67**, 133–141 (1999).
- <sup>20</sup>C. F. Gauss, Letter to Encke dated 24 December 1849 in *Werke*, Vol. II (Gedruckt in der Dieterichschen Universitäts Druckerei) (W. F. Kaestner, 1863), pp. 444–447. The relevant portion of this letter is quoted in Ref. 26, pp. 53–54.
- <sup>21</sup>J. Hadamard, “Sur la distribution des zéros de la fonction  $\zeta(s)$  et ses conséquences arithmétiques,” *Bull. Soc. Math. France* **24**, 199–220 (1896); C. J. de la Vallée Poussin, “Recherches analytiques sur la théorie des nombres premiers,” *Ann. Soc. Sci. Bruxelles* **20**, 183–256 (1896).
- <sup>22</sup>G. Mussardo, “The quantum mechanical potential for the prime numbers,” cond-mat/9712010.
- <sup>23</sup>For a detailed discussion of the Riemann zeta function see H. M. Edwards, *Riemann’s Zeta Function* (Dover, New York, 2001).
- <sup>24</sup>L. Euler, “Variae observationes circa series infinitas,” *Comm. Acad. Sci. Petropolitanae* **9**, 160–188 (1737). Euler’s proof of this formula is also presented in Ref. 26, pp. 102–107.
- <sup>25</sup>Julian Havil, *Gamma: Exploring Euler’s Constant* (Princeton U.P., Princeton, NJ, 2003), pp. 249–254.
- <sup>26</sup>John Derbyshire, *Prime Obsession: Bernhard Riemann and the Greatest Unsolved Problem in Mathematics* (Plume, New York, 2004).
- <sup>27</sup>Dan Rockmore, *Stalking the Riemann Hypothesis* (Pantheon, New York, 2005); Marcus du Sautoy, *The Music of the Primes* (Harper Perennial, New York, 2004).
- <sup>28</sup>See EPAPS Document No. E-AJPIAS-74-019606 for a MATHEMATICA notebook containing code to carry out the computations described in this article. This notebook can be found at ([fsweb.berry.edu/academic/mans/timberlake/rmatrix/](http://fsweb.berry.edu/academic/mans/timberlake/rmatrix/)). This document can be reached via a direct link in the online article’s HTML reference section or via the EPAPS homepage (<http://www.aip.org/pubservs/epaps.html>).
- <sup>29</sup>Hans-Jürgen Stöckmann, *Quantum Chaos: An Introduction* (Cambridge U.P., New York, 1999); Linda E. Reichl, *The Transition to Chaos: Conservative Classical Systems and Quantum Manifestations* (Springer-Verlag, New York, 2004), 2nd ed.
- <sup>30</sup>([www.dtc.umn.edu/~odlyzko/zeta\\_tables](http://www.dtc.umn.edu/~odlyzko/zeta_tables)).



Oscillating Prism. A prism can be used to split a narrow beam of white light into a spectrum. Conversely, it can also be used to reverse the process. One way to do this is to produce a spectrum with a prism, and then blur it by rocking the prism. In this example, at the National Museum of American History at the Smithsonian Institution, the prism is rocked by turning the crank. (Photograph and Notes by Thomas B. Greenslade, Jr., Kenyon College)